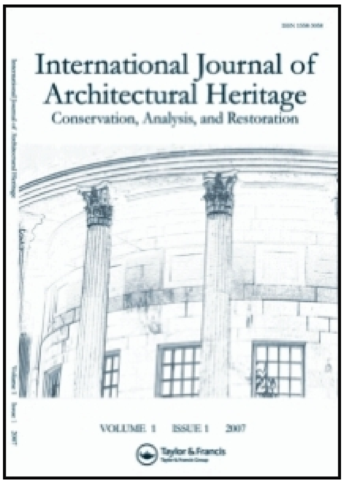

International Journal of Architectural Heritage
Publication details, including instructions for authors and subscription information:
http://www.informaworld.com/smpp/title~content=t741771160

Wooden Roof Box Structure for the Anti-Seismic Strengthening of Historic Buildings

Ezio Giuriani[a]; Alessandra Marini[a]
[a] Department of Civil, Architectural, Environmental and Land Planning Engineering (DICATA), University of Brescia, Brescia, Italy

To cite this Article Giuriani, Ezio and Marini, Alessandra(2008) 'Wooden Roof Box Structure for the Anti-Seismic Strengthening of Historic Buildings', International Journal of Architectural Heritage, 2: 3, 226 — 246

To link to this Article: DOI: 10.1080/15583050802063733

URL: http://dx.doi.org/10.1080/15583050802063733

International Journal of Architectural Heritage, 2: 226–246, 2008

ISSN: 1558-3058 print / 1558-3066 online
DOI: 10.1080/15583050802063733

WOODEN ROOF BOX STRUCTURE FOR THE ANTI-SEISMIC STRENGTHENING OF HISTORIC BUILDINGS

Ezio Giuriani and Alessandra Marini
Department of Civil, Architectural, Environmental and Land Planning Engineering (DICATA), University of Brescia, Brescia, Italy

A wooden roof strengthening technique aimed at transforming the roof pitches into anti-seismic shear-resisting diaphragms is presented in this article. Shear diaphragms gather and transfer the seismic loads to the shear-resisting walls. Diaphragms are built on top of the existing structures without significantly modifying the roof overall layout. The proposed strengthening technique is mainly reversible, minimally impairing the building integrity, and can be easily applied for the construction of anti-seismic wooden roofs in new buildings. A simplified design approach is presented, which allows identification of the static role of each element. An analytical method for the estimate of the box structure displacements, as well as a short digression on the displacement control requirements is also illustrated. The diaphragm technique was recently applied for the anti-seismic retrofit of some monumental buildings in Italy. A few case studies, as well as the basic design criteria for applying this technique are presented in this article.

KEY WORDS: seismic strengthening, historical buildings, wooden roof, strengthening technique, box structure

1. INTRODUCTION

Experience in the assessment and restoration of historical heritage has been carried out in Italy, especially in the past three decades. The survey of buildings, which were damaged or collapsed after recent earthquakes, improvement of the understanding of the structural behavior of ancient masonry structures undergoing seismic actions and highlighted the inadequacy of some strengthening solutions, especially those implying floor and roof strengthening with significant self-weight increase.

The structural response of historical buildings subjected to earthquake loads depends on many factors, such as the overall plan layout, the distribution, typology, interconnection and texture of the masonry walls, the location and size of openings, the occurrence of thrusting arches and vaults, and the typology of the roof, as well as the floor-to-wall and roof-to-wall mutual connections. As a result, failure mechanisms are not straightforward, and they are usually particular for each building (D'Ayala et al., 2002). Nevertheless, the most recurrent collapses and damages observed following recent seismic events frequently involved perimeter wall overturning (Figure 1a-c)

Received 13 July 2007; accepted 9 March 2008.
Address correspondence to Ezio Giuriani, Department of Civil, Architectural, Environmental and Land Planning Engineering (DICATA), University of Brescia, via Branze 43, 25123, Brescia, Italy. E-mail: egiuria@tin.it

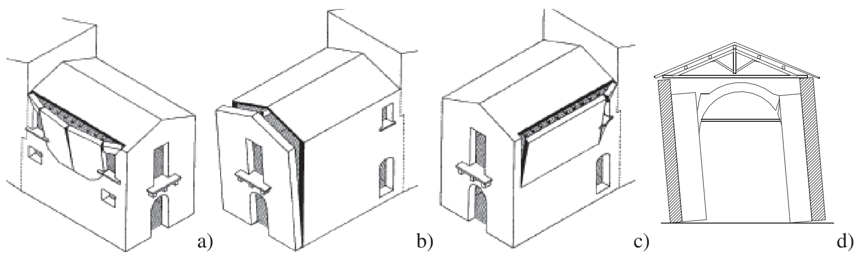

Figure 1. Schematic illustration of (a, b, c) wall overturning (De Benedectis et al., 1993) and (d) rocking of transverse arch pillars.

and, in some churches, the rocking of the transverse arch pillars (Figure 1d). The pillar-rocking motion induced large differential displacements between neighboring diaphragm-arches, thus resulting in severe damages to the possible nave vaults. It is worth noting that, following the strong earthquake in the Benaco area in northern Italy in year 2004, these unconstrained differential displacements were recognized as the major cause of the ruin of the nave vaults of two churches.

Global peripheral wall overturning and excessive pillar rocking occurred when the floors, the roof and the possible peripheral ties provided insufficient confinement of the toppling seismic action, which was eventually further increased by the horizontal thrust of the wooden roof (Figure 1a, c).

In order to improve the seismic resistance of ancient buildings, different earthquake-resistant features are traditionally proposed, namely: perimeter ties or floor diaphragms. Perimeter horizontal steel ties are inadequate in the case of unfavorable length-to-thickness ratios of the transversally loaded masonry walls. In this scenario, floor and roof diaphragms are frequently proposed against peripheral wall overturning to improve the seismic resistance (Giuriani and Marini, 2002; Giuriani, 2004). In the case of churches or in the case of buildings having at-sight wooden roofs, only roof diaphragms can be arranged.

In this article, the box structure solution is addressed with concern to the formation of thin roof diaphragms. The roof pitches are transformed into folded plates, which gather and transfer the roof seismic action to the shear resisting walls. In the case of long-span buildings lacking cross walls, in addition to the roof actions, the box structure also has to resist to the seismic action of both lateral crowning walls and possible diaphragm arches.

Finally, it is worth noting that the roof and floor diaphragm solutions are effective and suitable to avoid the most significant collapse modes, involving both the peripheral wall overturning and, in churches, the free or excessive rocking of the diaphragm-arch pillar system. Note that the limitation of rocking is needed to avoid any damage to the vaults due to shear deformation. Conversely, this solution may be ineffective against other failure modes, such as the wall in-plane shear sliding or the masonry out-of-plane collapse along the interstory height and between the cross walls (Magenes and Calvi, 1997; Griffith et al., 2003). Despite this deficiency, the roof and floor diaphragm solution may be adopted to repair and upgrade a great number of vulnerable buildings provided that the wall in-plane shear sliding, as well as masonry interstory out-of-plane collapse modes are less frequent and triggered by very strong earthquakes only.

The main objective of this article is to clarify the neither simple nor intuitive behavior of the roof pitch diaphragms. The article aims at clarifying the static role and the relevance of each structural member and the connections between the box structure and the masonry walls in order to provide useful guidelines for the correct structure proportioning. The simplified analytical method, discussed in the following paragraphs, is proposed as a useful tool for the understanding of the structure conception, rather than as an alternative to refined numerical approaches, such as the finite element method or the classical folded plate theory (Timoshenko, 1989).

In order to form the pitch diaphragms, the techniques, which are commonly developed and used for the flexural strengthening of wooden floors, can be addressed (Giuriani, 2004). Among these techniques, the solution of the thin ordinary concrete slab (50 mm), which is largely adopted to strengthen the existing wooden floors (Piazza and Turrini, 1983; Giuriani and Frangipane, 1993), might be unsuitable for the roof strengthening due to the significant weight increase (Figure 2a). Lighter solutions using a very thin slab of high performance concrete (Meda and Riva, 2001, Figure 2a), or thin steel plates (Giuriani and Plizzari, 2000, Figure 2b) could be preferred on the static point of view, but do not generally meet the restoration requirements.

The solution of the wooden diaphragms is usually preferred as it avoids a significant increase in the structural weight and thus in the seismic action. Roof diaphragms can be formed by placing overlaying plywood panels on the existing wooden planks (Giuriani 2004; Giuriani et al., 2005, Figure 2c). Plywood panels are connected to each other by means of nailed steel flanges. The whole pitch diaphragms are nailed to the perimeter steel chords, and to both roof rafters and masonry walls by means of steel studs and vertical anchored bars.

Alternatively, the pitch diaphragms can be arranged by superimposing new thick planks that are fastened together by means of horizontal studs embedded alongside neighboring boards (Giuriani et al., 2005, Figure 2d). The efficiency of this

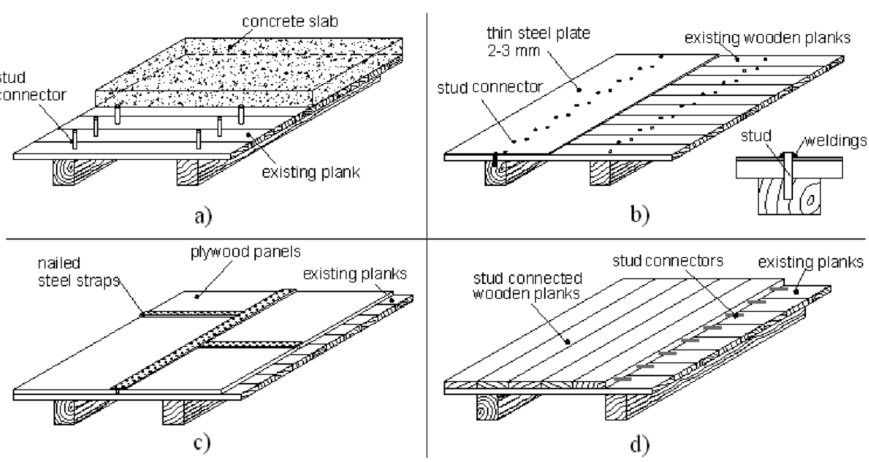

Figure 2. Schematic illustration of wooden floor in-plane shear strengthening by means of overlaying: (a) thin ordinary concrete slab; (b) thin steel plate; (c) nailed plywood panels; and (d) stud connected wooden planks.

technique was proven experimentally, but further refinements are needed for the technology to be applied in the construction practice. Note that this solution may be regarded as an enhancement of the orthogonal wooden plank technique proposed by Benedetti (1981).

2. DESIGN CRITERIA

This study focuses on gable roofs with reference to regular and long spanned buildings subjected to transverse horizontal actions. Small adjustment are needed for the proposed approach to be applied to different saddle roof typologies, namely with or without hipped shaped ends (Giuriani and Marini 2002).

The study investigates the effectiveness of the roof box-structure in improving the seismic behavior of ancient buildings, especially against the peripheral wall overturning and diaphragm arch pillar rocking. Focusing on the roof box structure, the article primarily aims at identifying the principal structural components, as well as their static role by means of a simplified approach.

The proposed simplified analytical method stems from the classical aeronautical structural analysis of ribbed panels, which is based on the assumption that the in-plane bending moment and the shear force be decoupled and resisted by the chords and panels, respectively (Bruhn, 1973). Considering a gable roof, the ribbed panels are not planar and behave like a box structure. The main structural elements composing the box structure are: the pitch-panel (Figure 3, point 1), the eaves chords (Figure 3, point c_{13}), the head gables (Figure 3, point 2), and the vertical ties embedded along the head gable and the lateral walls. The eaves chords and the pitch panels withstand the global horizontal bending moment and shear induced by the seismic action, respectively. Head gable walls transfer the seismic action to the foundations, and vertical ties avoid the roof uplift.

Seismic assessment requires not only assurance of the structure-bearing capacity but also the deformation control, especially in the case of free arch pillar rocking. The following paragraph focuses on the analysis of the structural behavior and conception. A further section provides some remarks about the deformation control.

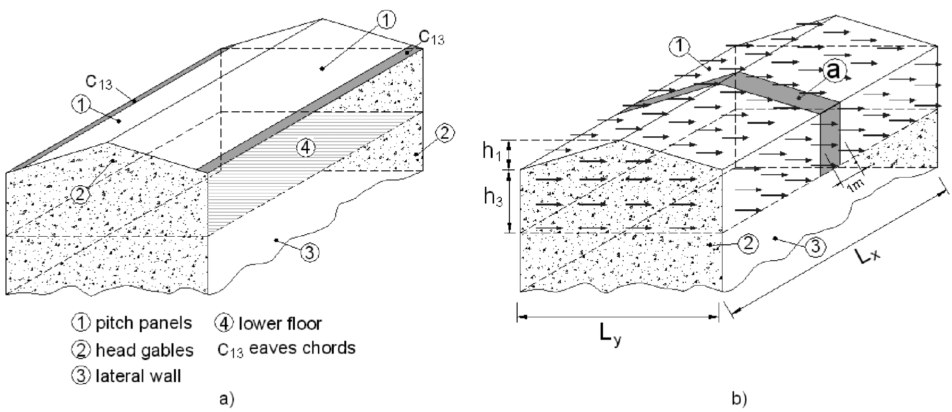

Figure 3. Schematic illustration of a) structural elements for the wooden roof strengthening, and b) seismic action distribution.

2.1. Box Structure Behavior and Resistance

The design of the roof box structure is based on the idea that the horizontal seismic actions of both lateral walls, the diaphragm-arches, and the roof are transferred by the roof box structure to the shear resisting head walls. Vertical loads are not considered because they are supposed to be supported by other structural systems, such as wooden trusses and ridge and wooden principal beams.

The pitch rafter-to-wall as well as the rafter-to-rafter constraints along the roof ridge are modeled as hinged. The same conservative assumption is made for the perimeter wall footings. Furthermore, the lower floor (Figure 3, point 4), the head shear walls and the head gables (Figure 3, point 2) are assumed to behave like in-plane rigid diaphragms.

In this scenario, in order to study the structure behavior, a two-step approach is addressed. In the first step vertical and horizontal idealized additional constraints are introduced along the roof ridgeline. In the second step these provisional constraints are removed and their reaction forces are backed out. In the first step, the unit-width stripe (Figure 3a), with additional vertical and horizontal constraints, undergoing seismic actions p_1 and p_3, behaves like a frame (Figure 4a). Each element is subjected to axial force, bending moment and shear, which can be easily evaluated. Note that the wall elements resist the axial forces and bending moment by developing a sort of natural arch, whose resistance depends on the wall thickness and on the vertical confinement provided by the vertical loads.

In this phase, significant uplifting vertical force per unit length n_A arises along the top lateral wall, which is equal to:

$$n_A = (p_1 l_{12} h_1 + p_3 h_3 h_1) L_y - g_1^* l_{12}/2 \tag{1}$$

where g_1^* is the roof dead load per unit area, which is generally conservatively reduced to account for possible vertical load reduction induced by the vertical component of the seismic acceleration.

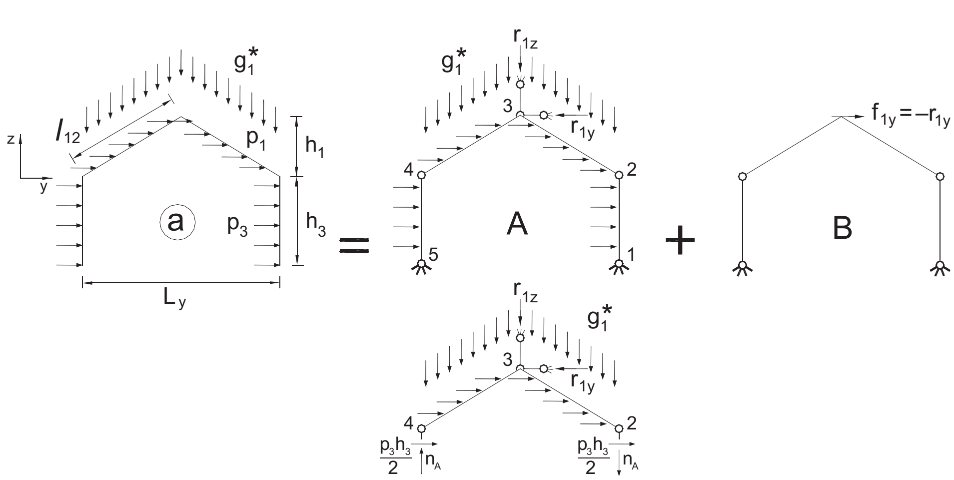

Figure 4. Illustration of frame-action.

When n_A is positive, the tensile forces must be balanced by the wall self-weight, through anchored bars, suitably embedded and distributed along the crowning masonries.

Shear forces v_A are transferred by the lateral walls to the roof box structure. Shear forces are equal to:

$$v_A = p_3 h_3 / 2 \tag{2}$$

In order to guarantee shear transferring between the crowning masonries and the box structure, suitable connections must be adopted.

In the second step, the additional ridge constraint reactions (r_{1y} and r_{1z}) are backed out with forces of equal intensity and opposite sign ($f_{1y} = -r_{1y}$, $f_{1z} = -r_{1z}$). The ridge vertical reaction f_{1z} is sustained by the ridge beam. Note that in case of symmetry, f_{1z} is only due to the dead loads $g_1{}^*$. Frame B is a free mechanism, thus unable to resist the horizontal force f_{1y}. For the balance to be restored, the box-structure must sustain these forces (Figure 5). In case of symmetry, equilibrium yields:

$$f_{1y} = 2p_1 l_{12} + p_3 h_3 \tag{3}$$

where l_{12} is the pitch width, and h_3 is the upper interstory height.

The roof box structure behaves like a simply supported beam undergoing distributed forces f_{1y} (Figure 6a). Equilibrium requires horizontal reactions R_y at the head gables. The horizontal forces f_{1y} and the reactions R_y are applied to the box structure shear centre, overlapping the ridgeline (Figure 6a), hence no torsion is introduced. This way, no vertical reactions, other than those generated in step 1 by the frame behavior (Equation 1), are added in step 2 along the eaves lines.

The eaves chord maximum axial forces F_{13} are obtained by the maximum bending moment M acting in the horizontal plane (Figure 6b). Axial forces F_{13} are equal to:

$$F_{13} = \frac{M}{L_y} = \frac{f_{1y} L_x^2}{8L_y} \tag{4}$$

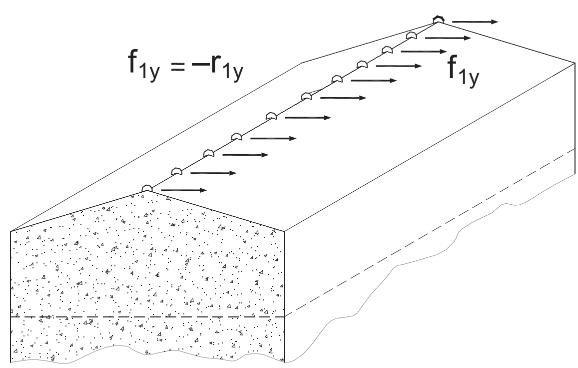

Figure 5. Illustration of horizontal ridge loads (f_{1y}) on box-structure.

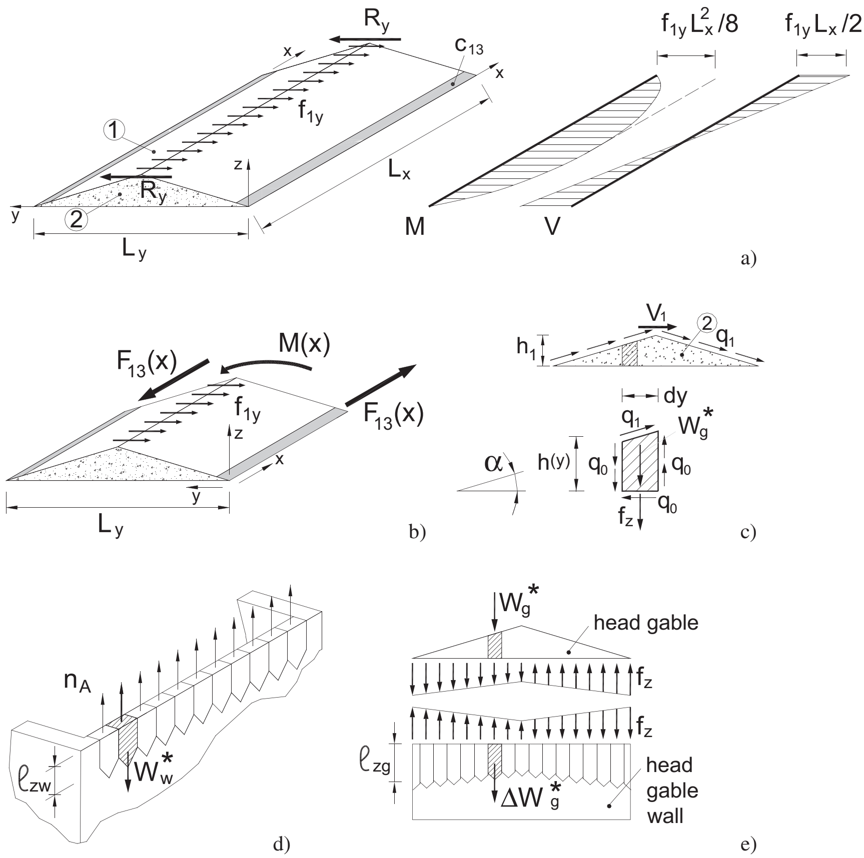

Figure 6. Simplified schemes for the evaluation of the force distribution in the box structure: a) roof box structure modeled as a simply supported beam, b) internal forces in the eaves chords, c) shear flow at the supports, d) uplift forces along the longitudinal walls, and e) uplift forces at the head gable support.

being L_y and L_x the distance between the center of the mass of the eaves chords and the box structure length respectively, and $M = (f_{1y}L_x^2)/8$ in case of uniformly distributed loads. The shear force is transferred by the two pitch diaphragms to the head gables (Figure 6c), and it is applied at the ridge level. In case of distributed loads, the shear force is equal to:

$$V_1 = \frac{f_{1y}L_x}{2} \tag{5}$$

Note that, in case of lumped masses, as for example in the case of church diaphragm arches, bending moment and shear force expressions must be appropriately modified.

The shear flow along the diaphragm cross section is equal to:

$$q_1 = \frac{V_1}{2}\left(\frac{L_y}{2\cos\alpha}\cos\alpha\right)^{-1} = \frac{V_1}{L_y} \tag{6}$$

The inclined shear flow q_1 must be balanced by both horizontal shear flow q_0 and vertical forces per unit length f_z (Figure 6c). Equilibrium yields:

$$\begin{aligned} q_o &= \left(\frac{q_1}{\cos\alpha}\right)\cos\alpha = q_1 \\ f_z &= 2q_o\tan\alpha - w_g^* \end{aligned} \tag{7}$$

where α is the roof pitch slope; w^*_g is the effective confining vertical load provided by the head gable weight per unit length, which can be possibly reduced by the vertical component of the seismic acceleration, according to the assumption adopted in Equation 1. Note that forces per unit length f_z vary along the y-axis following the variation of w_g (Figure 6c), and are tensile forces along half of the head gable.

2.2. Structure Proportioning

The proposed box structure proportioning aims at guaranteeing the elastic behavior throughout the design seismic event. Nevertheless, the ductile behavior of the nailed connections, which are recognized as the weakest link of the structure, ensures a ductility resource at the ultimate limit state.

The eaves chords are designed to resist the axial forces F_{13} (Equation 4). In the case of plywood pitch diaphragms, the eaves chords are over-proportioned to ensure their elastic behavior up to the structure collapse. To this end a conservative value for the steel design resistance should be preferably chosen. Steel design resistance can be set equal to one third of the yielding strength. Furthermore, in order to avoid eaves chord buckling, suitable confining screws in addition to the nails must be adopted.

The pitch panel thickness, the panel mutual connection, as well as the diaphragm connections to both the head gables and the eaves chords are proportioned to resist the maximum shear flow q_1 (Equation 6).

The nail spacing Δx_n along every steel flange, both in x and y directions, is equal to:

$$\Delta x_n = \frac{V_n}{q_1} \tag{8}$$

being V_n the design resistance of the single nail. Identical nail spacing has to be adopted for the panel-to-eaves chord connection. Experimental tests were performed on specimens obtained with high strength steel nails with a 4-mm diameter, 2-mm thick steel flanges and 27-mm thick plywood panels. The experimental ultimate nail resistance was approximately equal to $V_{nu} \cong 3$kN (Figure 7).

Distributed vertical anchor bars embedded along the head gable crowning masonries might be needed to prevent the roof uplift caused by the forces per unit length f_z (Equation 7). The same scenario occurs along the lateral walls when force per unit length n_A is positive (Equation 1). The distributed anchor bar embedment length ℓ_{zg} and ℓ_{zw} (Figure 6d-e) must be sufficient to allow balancing the weight w_w and ($w^*_g + \Delta w^*_g$) of the “lifted masonry”.

In order to transfer the shear force v_A (Equation 2), thus preventing the wall overturning, pitch diaphragm-to-wall steel dowel connections can be adopted. The

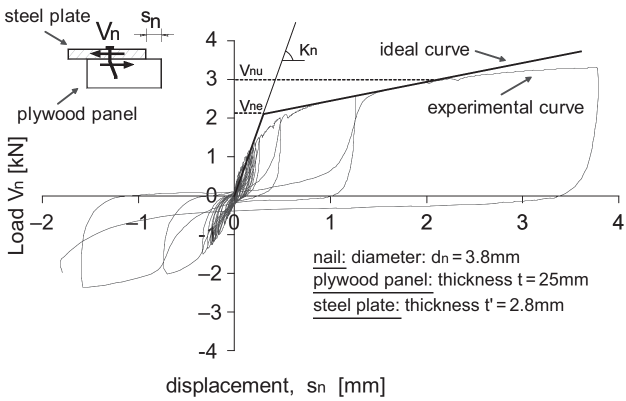

Figure 7. Experimental shear force versus slip cyclic relationship for the single nail connection.

dowel length has to be proportioned to avoid shear sliding of the lateral wall crowning masonries (Gattesco and Del Piccolo, 1998; Giuriani 2004; Tengattini et al., 2006).

2.3. Deformation Control for Plywood Structures

The appraisal of the roof structure horizontal displacements might be necessary anytime deformation restrictions must be enforced to avoid damages to the underlying masonry structures. Perimeter walls can usually endure large out-of-plane displacements without serious damages. In this case the diaphragm resistance must be guaranteed, whereas deformation control might be redundant. In other cases, i.e., in churches, deformation control may be necessary to prevent excessive in-plane shear deformability of the masonry vaults and/or excessive drift of the arch-diaphragm pillars.

Damages due to the excessive in-plane shear deformation of the nave vaults were frequently surveyed in many churches, as a result of the rocking-induced differential movements between the first diaphragm arch and the facade, as well as between the triumphal and the adjacent diaphragm arches. Unconstrained differential displacements produced by the strong rocking of the diaphragm arch pillars caused the ruin of the vault of the first nave bay and serious damages to that of the last bay in San Pietro Church (Roè Volciano, Brescia, Italy) during the earthquake of year 2004.

As for the diaphragm-arches, deformation control is necessary to avoid excessive displacements induced by the pillar rocking, which can result in damages and masonry crushing at the pillar base. To restrain the deformability of the box structure, over-proportioned elements, as well as over-proportioned connections should be adopted. In the following, an analytical model for the evaluation of the horizontal deformability of the plywood box structure is proposed.

2.4. Acceptable Horizontal Deformation

The roof box structure deformation must be restrained to prevent damages to the underlying vaults. The estimate of the vault allowable horizontal shear deformation is a

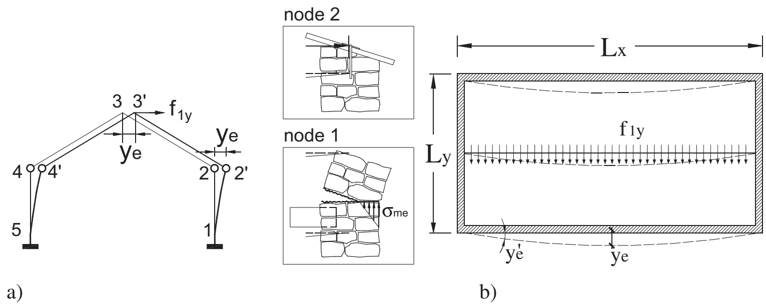

Figure 8. a) Illustration of the vertical wall drift when the structure is subjected to horizontal loads, and the details of the wall footing (node 1) and top edge constraint to the roof pitch diagrams (node 2), and b) transverse deflection of the roof box structure undergoing the ridge horizontal loads.

difficult task; nevertheless, lacking a more refined evaluation, a tentative shear deformation value $\gamma^* \leq 0.25\% \div 0.5\%$ is proposed in this article. Accordingly, the slope of the box structure transverse deflection at the head gable supports y'_e (Figure 8b) has to be smaller than the maximum shear deformation γ^* allowed by the vault:

$$\gamma'_e \leq \gamma* \tag{9}$$

The suggested shear deformation range was obtained by reference to a thin panel undergoing pure shear and by assuming in case of smeared cracks an average elongation of the panel diagonal undergoing traction equal to $0.15\% \div 0.3\%$. The estimate of the average elongation was obtained by assuming an acceptable crack opening of $7.5 \div 15$mm during the earthquake and by referring to the diagonal crack pattern observed in some churches damaged by the earthquake (San Pietro Church). Note that more research should be performed to achieve a sound evaluation of the vault maximum shear deformation.

When displacement control is required to prevent damages to the diaphragm-arch pillars, the allowable box structure transverse deflection has to be compatible with the maximum drift of the diaphragm arch pillars. Lacking a refined evaluation, a maximum drift d_e ranging between $1 \div 2\%$ is here adopted (Figure 8a). Accordingly, when subjected to earthquake loadings, the roof box structure lateral deflection y_e (Figure 8b) has to be equal to or smaller than the displacement y_{ew} allowed by the drift of the pillars:

$$y_e \leq y_{ew} \tag{10}$$

where: $y_{ew} = d_e h_3$ (Figure 8a).

2.5. Evaluation of the Box Structure Deformations

In case of uniformly distributed transverse force f_{1y}, the box structure transverse deflection is obtained by accounting for flexural and shear deformability. The maximum slope and deflection of the box structure (y'_e and y_e) can be evaluated by addressing the principle of virtual works, which yields:

$$y_e = \left[\frac{5}{384}\frac{f_{1y}L_x^4}{E_w^* J_{id}} + \frac{f_{1y}L_x^2}{8G_w^* L_y\ t\cos\alpha}\right] \tag{11}$$

$$y'_e = f_{1y}\left[\frac{1}{24}\frac{L_x^3}{E_w^* J_{id}} + \frac{L_x}{2}\frac{1}{L_y t}\frac{1}{G_w^*}\right] \tag{12}$$

where E^*_w and G^*_w are the pitch diaphragm equivalent Young and shear moduli, which account for the shear deformability of the panel nail connections; J_{id} is the second moment of area of the ideal transformed cross section; t is the plywood panel thickness. Chords and pitch diaphragm stiffness is assumed to be constant along the x-axis.

The deformability of the box structure is strongly affected by the shear slip of the nailed connections. In order to account, in a simple fashion, for the reduction of the bending and shear stiffness caused by the panel-to-panel nailed connections, equivalent Young (E^*_w) and shear (G^*_w) moduli are adopted in Equation10 and 11.

The equivalent shear modulus (G^*_w) can be evaluated by reference to the panel stripe pertaining to each nail (having width Δx_n) illustrated in Figure 9a. The total shear displacement s_{tot} between adjacent plywood panels is given by the addition of the nail slip s_n and the elastic wood panel shear deformation γ_w:

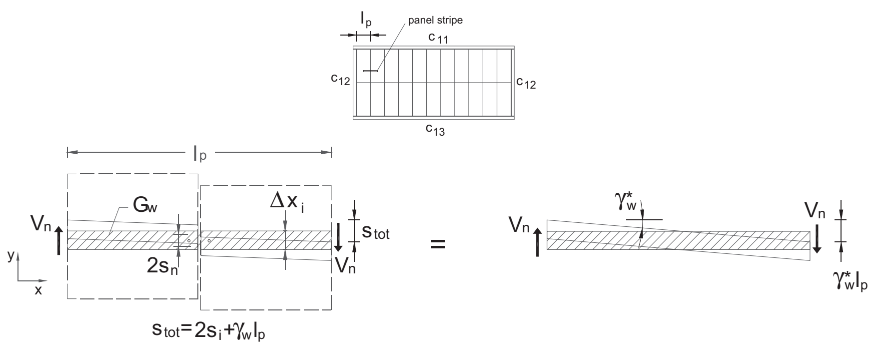

a)

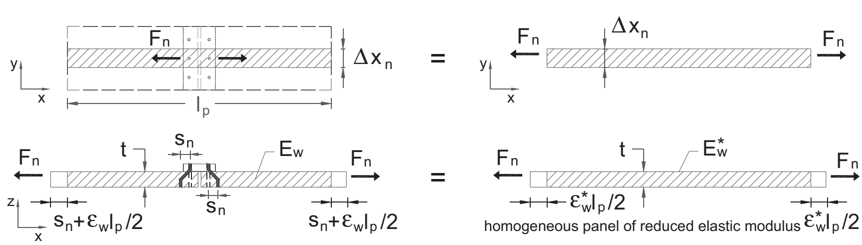

b)

Figure 9. Simplified evaluation of modified equivalent (a) shear modulus (G^*_w); and (b) the Young modulus (E^*_w).

$$s_{tot} = 2s_n + \gamma_w l_p \tag{13}$$

being l_p the panel width.

The connection shear slip s_n is given by the elastic relationship:

$$s_n = V_n / k_n \tag{14}$$

where k_n is the single nail shear stiffness (Figure 7, branch $s_n < s_{ne}$), which can be obtained either experimentally, or by reference to formulations provided by the literature ().

The ideal shear deformation γ^*_w is:

$$\gamma^*_w = \frac{s_{tot}}{l_p} \tag{15}$$

Being $\tau_w = V_n / A_{wn}$ and $\gamma_w = V_n / (A_{wn} G_w)$, by substituting Equation 12 and 13 in Equation 14, the ideal shear modulus $G^*_w = \tau_w / \gamma^*_w$ becomes as follows:

$$G^*_w = \frac{k_n l_p}{2A_{wn} + \frac{k_n l_p}{G_w}} \tag{16}$$

where $A_{wn} = \Delta x_n t$ is the panel stripe cross section area, Δx_n is the nail spacing and t is the panel thickness.

The equivalent Young modulus (E^*_w) is evaluated by considering the unit panel stripe in Figure 9b. The total displacement caused by the tensile force (F_n) across the panel stripe is equal to:

$$2s_n + \varepsilon_w l_p = \varepsilon^*_w l_p = \frac{F_n}{A_w E^*_w} l_p \tag{17}$$

being ε_w and ε^*_w the plywood panel and the equivalent panel axial strains, respectively.

By rearranging Equation16, the equivalent Young modulus (E^*_w) can be obtained:

$$E^*_w = \frac{k_n l_p}{2A_{wn} + \frac{k_n l_p}{E_w}} \tag{18}$$

Note that the plywood deformability plays a significant role in the appraisal of the equivalent panel characteristics. By neglecting the panel deformability — i.e., by setting E_w and G_w equal to infinity in Equation 15 and Equation 17, and by assuming ordinary values of the geometric and mechanic properties ($l_p = 1200$ mm, $A_{wn} = 50$ mm·27.5mm, $E_w = 5000$ MPa, $G_w = 2500$ MPa, $k_n = 2700$ N/mm) — a 25% overestimate of the ideal Young modulus E^*_w and a 50% overestimate of the shear modulus G^*_w are obtained.

3. CASE STUDY

The proposed simplified analytical formulation is applied to the design of the anti-seismic retrofit of a typical gable roof (Figure 5). Roof and crowning masonry wall seismic loads are carried by the box structure, overlaying the existing roof.

With reference to Figure 3, the following data are given: $L_x = 30.0$ m; $L_y = 10.0$ m; $h_1 = 2.02$ m; $h_3 = 3.0$ m; $l_{12} = 5.39$ m; $\alpha = 22°$. The roof pitch seismic action is set equal to 20% of the vertical load ($g_1 = 3$ kN/m^2), thus $p_1 = 0.6$ kN/m^2. The lateral wall seismic action is equal to $p_3 = 2$ kN/m^2, where a wall thickness $s_m = 0.5$ m and a specific gravity load $g_m = 20$ kN/m^3 are assumed.

The horizontal forces f_{1y} applied along the box structure ridgeline (Equation 3) are equal to:

$$f_{1,y} = 2p_1 l_{12} + p_3 h_3 = 12.5\text{kN/m} \tag{19}$$

The box structure maximum bending moment M and shear force V are equal to:

$$M = \frac{f_{1y} L_x^2}{8} = 140\text{kNm} \quad V_1 = \frac{f_{1y} L_x}{2} = 187.5\text{kN} \tag{20}$$

The eaves chord axial forces F_{13} and cross section area yield as follows:

$$F_{13} = \frac{M}{L_y} = 140.6\text{kN} \quad A_{c_{13}} = \frac{F_{13}}{\sigma_s} = 1125\ \text{mm}^2 = 75 \times 20\ \text{mm}^2 \tag{21}$$

where a reduced value of the steel design resistance is adopted ($\sigma_s \cong 100$ MPa) to prevent buckling.

In order to avoid the compressed chord uplift induced by instability, anchorages and screws fixing the chord to the wall and to the wood panels are needed. The maximum anchorage spacing Dx_a depends on the thickness of the chords. The adopted reduced steel stress value $\sigma_s = \chi f_{yd} \cong 100$ MPa yields an instability reduction factor $\chi = 0.35$ (for $f_{yd} = 280$ MPa). This reduction factor corresponds to a slenderness approximately equal to $\lambda \cong 120$. The effective length is equal to:

$$l_o = \lambda \frac{t_c}{\sqrt{12}} = \frac{120 \cdot 20}{\sqrt{12}} \cong 0.7\ \text{m} \tag{22}$$

being $t_c = 20$ mm the thickness of the eaves chord steel plate.

The maximum anchorage spacing Dx_a, yields as follows:

$$\Delta x_a = 2l_o = 1.4\ \text{m} \quad l_o = \lambda \frac{t_c}{\sqrt{12}} = \frac{120 \cdot 20}{\sqrt{12}} \cong 0.7\ \text{m} \tag{23}$$

The maximum shear flow q_1 and the nailed connection spacing Dx_n are respectively equal to:

$$q_1 = \frac{V_1}{L_y} = 18.75\ \text{kN/m} \quad \Delta x_n = \frac{V_n}{q_1} = 53\ \text{mm} \rightarrow 50\ \text{mm} \tag{24}$$

where high strength steel nails of 4 mm diameter with a resistance $V_n = 1.0$ kN are adopted. Similar nailed connections are used to fix the wood panel to the eaves chords.

Pitch diaphragms undergoing the shear flow q_1 are made of commercial plywood panels having a thickness t = 27.5 mm. The maximum shear stress is equal to:

$$\tau_w = \frac{q_1}{t} = 0.68\text{MPa} \tag{25}$$

The pitch diaphragm-to-head gable dowel connections are subjected to the shear flow q_1, thus the dowel spacing is equal to:

$$\Delta y_d = \frac{V_{dn}}{q_1} = \frac{6.0}{18.75} = 0.32 \text{ m} \tag{26}$$

being $V_{dn} = 6$ kN the plywood panel-to-masonry wall connection design resistance, corresponding to 1/2 of the smallest ultimate resistance recorded in the experimental tests on a 16 mm diameter steel stud (Gattesco and Del Piccolo, 1998, Giuriani, 2004; Tengattini et al., 2006).

The maximum embedment length l_{zg} of the vertical anchorages placed along the head gable is equal to (Figure 6e):

$$l_{zg} = \frac{f_z}{s_m \gamma_m} = \frac{15.15}{0.5 \cdot 20} = 1.5 \text{ m} \tag{27}$$

being $f_z = 2q_o \tan\alpha = 2.0 \times 18.75 \times 0.4 = 15.15$kN/m, where w_g is conservatively neglected.

The uplift distributed forces n_A induced by the frame behavior along the lateral walls are equal to:

$$n_A = (p_1 l_{12} h_1 + p_3 h_3 h_1)/L_y - g_1^* l_{12}/2 = -3.5\text{kN/m} \tag{28}$$

where the dead loads are conservatively reduced to 70% ($g^*_1 = 0.7g_1 = 2\text{kN/m}^2$) to account for possible vertical load reduction induced by the seismic acceleration vertical component. Note that in this case no anchorages are needed, provided that n_A is negative, thus box structure uplift is inhibited.

The transverse shear force v_A transferred by the lateral walls to the box structure is equal to:

$$v_A = p_3 h_3/2 = 3\text{kN/m} \tag{29}$$

To allow shear transferring, wall-to-pitch diaphragm dowel connections are required. The dowel connection spacing is equal to:

$$\Delta x_d = \bar{V}_{dn}/v_A = 3/3 = 1 \text{ m} \tag{30}$$

where a reduced value of the dowel resistance is adopted to account for the reduced out-of-plane shear resistance of the top wall ($V_{dn} = 3$kN, corresponding to 1/4 of the smallest ultimate resistance recorded in the experimental tests on a 16-mm diameter stud, having an embedment length of 0.3 ÷ 0.5m; Tengattini et al., 2006). Note that this distance is smaller than spacing Dx_a required to avoid eaves chord buckling. Therefore, by enforcing this spacing to the connections along the lateral walls, instability is inhibited.

As for the structure deformation, by setting $E_w = 5000$ MPa and $G_w = 2500$ MPa, Equation 15 and Equation 17 yield $G^*_w = 800$ MPa and $E^*_w = 953$ MPa, respectively. The maximum in-plane pitch diaphragm displacement is equal to (Equation 10):

$$y_e = \frac{5}{384}\frac{f_{1y}L_x^4}{E_w^* J_{id}} + \frac{f_{1y}L_x^2}{8G_w^* L_Y t \cos\alpha} = 7.3 + 13.7 = 21.0 \text{ mm} \tag{31}$$

where $J_{id} = 1.88 \cdot 10^{13}$ mm^4.

The deflection assessment reads as follows:

$$y_e = 21.0 \text{ mm} \le d_e h_3 = 0.01 \cdot 3000 = 30 \text{ mm} \tag{32}$$

The requirement of Equation 9 is therefore largely satisfied.

The slope of the box structure deflection at the head gable supports y'_e is equal to:

$$y'_e = f_{1y}\left[\frac{1}{24}\frac{L_x^3}{E_w^* J_{id}} + \frac{L_x}{2}\frac{1}{L_y t}\frac{1}{G_w^*}\right] = 2.25 \cdot 10^{-3} \le y'_{ew} \tag{33}$$

This value satisfies the requirement of Equation 8.

3.1. Numerical Assessment

The static behavior of the gable roof box structure analyzed in the case study, which was proportioned and studied by reference to the simplified method, was compared with the results of linear elastic finite element analyses. Equivalent static transverse seismic action was considered. In the analyses, only the roof was modeled; the lateral masonry walls were represented by vertical hinged beam elements, inhibiting any vertical displacement of the roof along the eaves lines, but allowing horizontal transverse displacements and rotations. The head gables were modeled as in-plane rigid diaphragms, allowing out-of the plane displacements and rotations.

Two different mesh types (A, B in the following) were analyzed (Giuriani et al., 2002): in mesh A (Figure 10a), all structural elements composing the existing wooden roof and the box structure were modeled. Wooden rafters and steel eaves chords were modeled by means of beam elements, whereas pitch web panels were modeled by means of plate elements. Wooden rafters were hinged at both ends. The deformability of the nailed shear connections between the pitch web panels was considered by introducing along every connection special plate elements having a reduced equivalent elastic E^*_w and shear moduli G^*_w. Reduced stiffness properties were obtained by reference to Equations 15 and 17. Geometric and mechanical characteristics of each element are those illustrated in Table 1a. Load distribution is shown in Figure 10a.

In mesh B (Figure 10b) the roof box structure was modeled without the wooden rafters. Only the ridge horizontal load f_{1y} was considered. The box structure was modeled as in mesh A. Geometric and mechanical characteristics of each element are

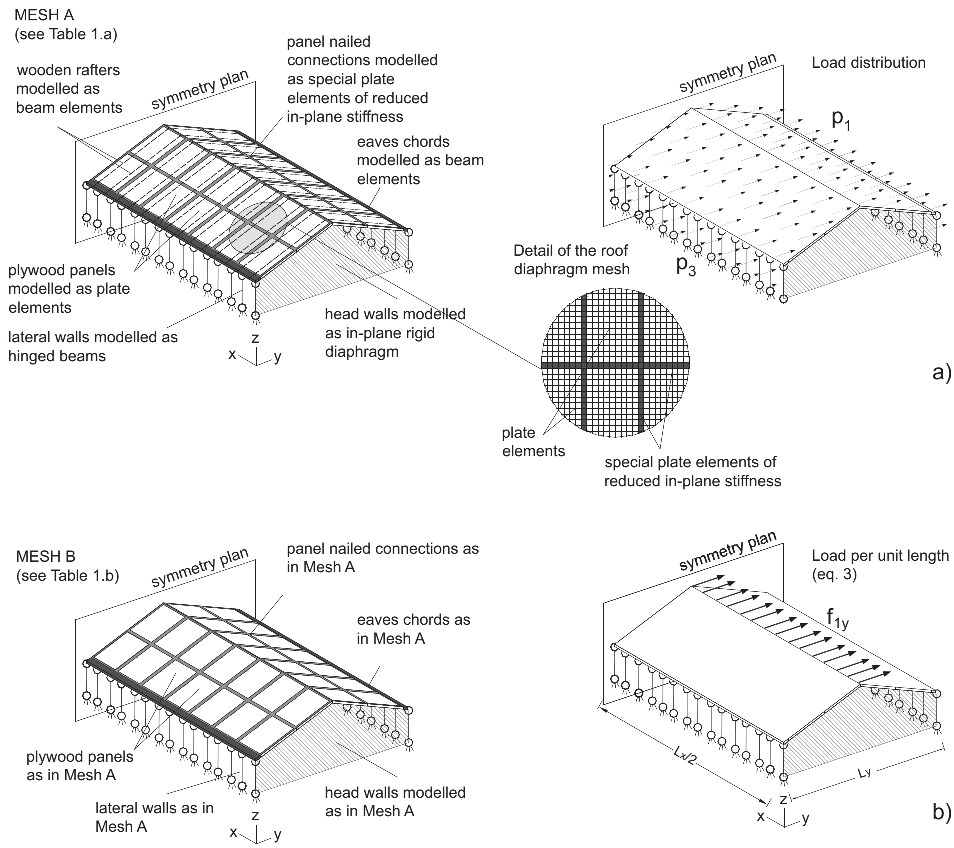

Figure 10. a) Numeric models accounting for all the box structure elements, for the existing wooden rafters, as well as the actual load distribution (Mesh A), and b) Simplified numeric model of the box structure only, with the ridge distributed load (Mesh B).

those illustrated in Table 1b. The analyses performed on mesh A and B showed similar results, proving that the wooden rafters do not appreciably influence the box structure behavior.

Table 2 shows the main results obtained by reference to either the simplified method or the numerical analysis. Theoretical and numerical results compare well in terms of maximum axial forces, horizontal displacements at the ridge mid-span, and slope of the box structure deflection at the head gable. The theoretical results slightly underestimated the numerical displacements and slightly overestimated the eaves axial forces. Details on the numerical study are illustrated in Giuriani et al. (2002).

4. ANTI-SEISMIC RETROFIT OF ANCIENT WOODEN ROOFS

The box structure solution has been applied for the anti-seismic retrofit of ancient wooden roofs of a few monumental buildings and churches in northern Italy. A brief description of the geometry and the main static problems of two case studies, as well as the addressed design criteria are illustrated in the following paragraphs.

Table 1. Mesh geometric and mechanical characteristics

Mesh A: a)	Mesh B: b)
Plywood web panel:	Same box structure of mesh A, without wooden rafters
Eight node PLATE elements:	Only equivalent horizontal loads per unit length along the ridgeline are assumed
$100 \times 100 \times 27.5$ mm $E_w = 5000$ MPa; $G_w = 2500$ MPa	
Panel-to-panel nailed connections:	
Special plate element of reduced stiffness	
Eight node PLATE elements:	
$100 \times 100 \times 27.5$ mm	
$E_w^* = 96$ MPa; $G_w^* = 94$ MPa according to Equation15 and Equation 17, where: $l_p = 100$mm, $\Delta x_n = 50$ mm,	
$A_{wn} = 1375$mm^2; $k_n = 2700$ N/mm, $E_w = 5000$MPa; $G_w = 2500$MPa	
Steel eaves chords:	
BEAM element: cross section $A_{11} = 75 \times 20$mm^2 $E_s = 210000$ MPa	
Roof wooden rafters:	
BEAM Elements: 140×200mm $E_w = 9000$ MPa	

Table 2. Comparison of analytical estimates and numerical results

	F_{13} [kN]	y_e'	y_e [mm]
Mesh A	128	$2.30\ 10^{-3}$	19.7
Mesh B	133	$2.67\ 10^{-3}$	20.3
Theoretical	140.6	$2.25\ 10^{-3}$	21

4.1. Structural Reinforcement of Calini ai Fiumi Palace in Brescia, Italy

The western wing of the Palazzo Calini ai Fiumi, new headquarters of the Law Department of the University of Brescia, was recently restored with the anti-seismic retrofit of the wooden roof. The two-layer building is composed by a porch at the ground floor, overlooking an internal courtyard and a large conference room on the first floor (10×30 m; interstory height of 7 m; Figure 11a). The conference room outer walls lack a transverse reinforcing structure preventing the out-of-plane displacements. Furthermore, the masonry wall facing the internal courtyard (labeled as *3)* in Figure 11a) is simply supported on the porch columns and is therefore not securely fixed to the ground. As for the roof, the inferior purlins are too slender to sustain seismic action pertaining to the wall.

The retrofit works were aimed at strengthening the existing wooden roof (labeled as *1)* in Figure 11a) and the main room floor (labeled as *4)* in Figure 11a) against seismic actions by applying overlying diaphragms on both structures. Note that given the large span of the masonry wall, the traditional perimeter ties would have been inadequate. The wall on the colonnade was strengthened with vertical steel bars

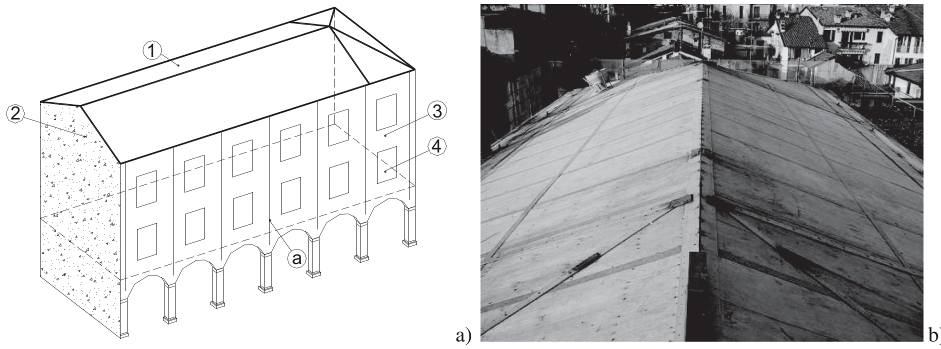

Figure 11. Palazzo Calini ai Fiumi: a) simplified scheme of the structure; b) photograph of the anti-seismic plywood roof box structure.

(labeled as *a)* in Figure 11a) built in the wall between the openings. This way the masonry was provided with sufficient strength and stiffness to transfer the seismic actions to the resisting diaphragm of both the main room floor and the saddle roof.

The floor and the roof were designed to resist and transfer both their seismic actions and those pertaining to the lateral walls to the shear resisting head gables (labeled as *2)* in Figure 11a). The floor diaphragm was obtained by casting a thin concrete slab on top of the existing wooden floor, whereas the pitch diaphragms were made of plywood panels connected by thin steel flanges nailed to the panels. Figure 11b shows a perspective view of the anti-seismic plywood roof box structure upon completion.

4.2. Structural Reinforcement of San Pietro Church in Roè Volciano, Brescia, Italy

San Pietro church (XIV century) is a single nave church, with lateral chapels covered by a gable roof (Figure 12a). The church has been largely remodeled and restored through the years to meet the new religious needs, but most of all to repair the severe damages caused by recurrent earthquakes, in the Benaco area.

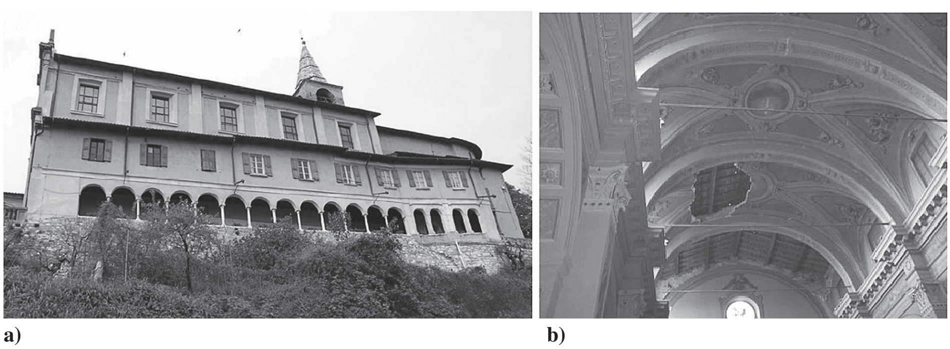

Figure 12. Photographs of the San Pietro Church in Roè Vociano, Brescia, Italy: a) prospective view of the southern front; and b) damage of the barrel vault of the first main nave bay.

Figure 13. Photographs of the San Pietro Church in Roè Vociano: general view and of the plywood roof box structure and detail of the eaves chord connected to the underlying masonry by means of steel studs and deep anchorages.

A series of four transverse arches divides the nave into 5 bays. The nave is covered by 50-mm, single-leaf, masonry barrel vaults. The existing gable roof, lacking any anti-seismic characteristics, is made of transverse rafters carried by four beams and the ridge beam. The last strong seismic event hitting northern Italy in 2004 caused the global ruin of the barrel vault close to the facade (Figure 12b), and the extended damage of the vault next to the triumphal arch. The damage was mainly caused by the excessive in-plane shear deformation induced by the unconstrained differential displacement of the facade and of the neighboring diaphragm arch. The differential displacements were the result of the pronounced difference in the stiffness of the vertical bearing structures.

Strengthening works concerned the reconstruction and repair of the ruined and damaged vaults. Furthermore, in order to avoid future damages to the masonry structures a plywood box structure was arranged (25×10m, Figure 13 a,b), adopting the same technique described in the previous case study.

5. FINAL REMARKS

Historic masonry buildings undergoing seismic actions frequently exhibit damages or collapses induced by the overturning of the perimeter walls and, in churches, by the rocking of the diaphragm arch pillars. Damages are usually more pronounced in long-span buildings lacking cross walls, as the wall span-to-thickness ratio is unfavorable and little constraint is provided to the toppling masonry walls. In these cases, existing or added peripheral ties are ineffective. In-plane shear resistant floor and roof diaphragms, transforming the building into a box-structure, can be a viable solution to avoid these mechanisms. The box structure gathers and transfers the seismic action to the shear resisting walls.

In this article, a wooden lightweight box structure is proposed, which is obtained by superimposing plywood panels to the existing wooden roofs. The proposed technique meets the requirements of the modern restoration principles, provided that it is mainly reversible and does not impair of the building integrity. As a further advantage, this technique adopts commercial materials, which can be easily acquired by the constructors. As a drawback, however, specialized man labor may be required.

The main focus of this research work is the static behavior and the resistance of the roof box structure. A simplified design approach was introduced, which allows clarification of the neither simple nor intuitive structural behavior and the static role of each box-structure component, as well as their interaction with the peripheral walls.

The proposed analytical model is useful not only for the understanding of the structural behavior and conception, but it can also be useful to give a reference for any eventual refined structural analysis. As a matter of fact, when addressing refined analysis methods, such as the FE method, the comprehension of the structural behavior is crucial for the correct modeling of the structure, as well as for the accurate and focused selection of the most critical element to be checked and verified. Furthermore, the estimate of the element internal forces obtained by means of the illustrated theory can be helpful to compare and validate the numerical results.

For the design of box structures it is important to take into account not only the global behavior, but also the detailing of every single component, their mutual interaction, and the connection of the roof to the underlying masonry walls. The box structure is designed to behave elastically throughout design seismic events. As a result, no energy dissipation capacity can be accounted for.

Provided that the design of roof diaphragms must guarantee resistance to allow the transferring of the seismic actions to the shear resisting walls, deformation restrictions might be sometimes enforced in order to avoid large transverse deflections of the roof, which could damage the underlying masonry walls and vaults. This problem was evidenced in some churches following the earthquake that struck northern Italy in 2004, when the unconstrained differential displacements between adjacent diaphragm arches were recognized as a major cause of the ruin of a nave vault.

Finally, it is worth noting that the introduction of the roof box structure modifies the dynamic behavior of the building. The evaluation of the actual seismic forces are strictly bound to the correct evaluation of the interaction between the existing resisting masonry walls and the roof box structure. The study of the dynamic behavior of the strengthened building is a compelling and challenging task, which is so vast that it requires further synergic work in different research fields. Such a study requires detailed and reliable modeling of every part of the structure, as well as of their mutual interaction, also accounting for correct modeling of the materials and of the earthquake ground motions. In this scenario, the future development of the research will be aimed at clarifying the role of the roof box-structure on the rocking of both the lateral walls and transverse diaphragm arches.

ACKNOWLEDGEMENTS

This work was developed within the research project DPC-ReLUIS 2005–2008, Research line n. 1: “Vulnerability assessment and anti-seismic strengthening of masonry buildings”. ReLuis and MURST financial contributions are gratefully acknowledged.

REFERENCES

Benedetti, D. 1981. Riparazione e consolidamento degli edifici in muratura. In *AA.VV. Costruzioni in zona sismica*, Cap. 11. Milano, Italy: Edizioni Masson.

Bruhn, E. F. 1973. *Analysis and design of flight vehicle structures*. Indianapolis, IN: Jacobs Publishing Inc.

D'Ayala, D., and Speranza, E. 2002. An integrated procedure for the assessment of seismic vulnerability of historic buildings [CD-ROM]. *Proceedings of the 12th European Conference on Earthquake Engineering*, paper n. 561 London, England: Elsevier Science.

De Benedectis, R., De Felice, G., and Giuffrè, A. 1993. Restauro antisismico di un edificio. In *Sicurezza e conservazione dei centri storici: Il caso Ortigia,* ed. Giuffrè A. Bari, Italy: Editrice Laterza, 189–205.

Eurocode 5. 2005. European Committee for Standardization (CEN). UNI EN 1995:2005. Design of timber structures. Brussels.

Gattesco, N., and Del Piccolo, G. 1998. Shear transfer between concrete members and stone masonry wall through driver dowels. *European Earthquake Engineering*, 1.

Giuriani, E., and Plizzari, G. 2000. Studio sperimentale sul comportamento dei solai in legno rinforzati con lastra in acciaio per resistere alle azioni sismiche. *V Workshop Italiano sulle Costruzioni Composte*, Polermo, November 23–24, 2000, 277–292.

Giuriani, E., and Frangipane, A. 1993. Wood-to-concrete composite section for stiffening of ancient wooden beam floors. *Atti del 1° Workshop Italiano sulle Strutture Composte*, Trento, Italy, June 17–18, 1993. Trento, Italy: Università degli studi di Trento.

Giuriani, E., and Marini, A. 2002. Coperture in legno antisismiche. *Technical Report*(6). Brescia, Italy: Università degli Studi di Brescia, Dipartimento di Ingegneria Civile.

Giuriani E., Guilarte F., Marini A., and Tonioli A. 2002. Comportamento sismico delle coperture in legno. *Technical Report*, (19). Brescia, Italy: Università degli Studi di Brescia, Dipartimento di Ingegneria Civile.

Giuriani E., Marini A., and Plizzari G. 2005. Experimental behavior of stud connected wooden floors undergoing seismic action. *Restoration of Buildings and Monuments* 11(1):3–24.

Giuriani, E. 2004. L'organizzazione degli impalcati per gli edifici storici. *L'Edilizia*. Speciale Legno strutturale (134): 30–41.

Griffith M. C., Magenes G., Melis G., and Picchi L. 2003. Evaluation of out-of-plane stability of unreinforced masonry walls subjected to seismic excitation. *Journal of Earthquake Engineering* 7(special issue 1): 141–169.

Magenes G., and Calvi G. M. 1997. In-plane seismic response of brick masonry walls. *Earthquake Engineering and Structural Dynamics* 26: 1091–1112.

Meda, A., and Riva, P. 2001. Strengthening of wooden floors with high performance concrete slabs. *International Journal for Restoration of Buildings and Monuments* 7(6):621–640.

Piazza, M., and Turrini, G. 1983. Il recupero statico dei solai in legno. *Recuperare* (7): 396–407.

Tengattini, C. G., Marini, A., and Giuriani, E. 2006. Connessioni a taglio nelle murature. *Tecnichal Report 3a.1-UR11-1 RELUIS — Progetto di ricerca N.1 — Vulnerability assessment and anti-seismic strengthening of masonry buildings* [In Italian].

Timoshenko S.P., and Woinowsky-Krieger S. 1989. *Theory of plates and shells*. New York: McGraw-Hill.